Theory of dynamic acoustic radiation force experienced by solid cylinders

Farid G. Mitri* and Shigao Chen
Ultrasound Research Laboratory, Department of Physiology and Biomedical Engineering, Mayo Clinic College of Medicine and Foundation, 200 First Street SW, Rochester, Minnesota 55905, USA
(Received 12 November 2003; published 12 January 2005)

A body insonified by a sound field is known to experience a steady force that is called the acoustic radiation force. This force can also be dynamic or oscillatory, knowing that the intensity of the incident sound field changes over time (amplitude modulation). The present paper develops the theory of dynamic radiation force experienced by a solid cylinder immersed in an ideal fluid. Analytical solutions of the equations for the dynamic force are derived. The equations provide analytical radiation force dependencies on the acoustic field and medium parameters. The case of compressional and shear waves' absorption in the solid material of the cylinder is also discussed. It is shown here that radiation force is no longer static and cannot be treated as a steady-state phenomenon.

DOI: 10.1103/PhysRevE.71.016306 PACS number(s): 43.25.+y

I. INTRODUCTION

The acoustic radiation force [1–13] is interpreted as the time-averaged force acting on an object in a sound field. This force is caused by a change in the energy density of an incident acoustic field. Thus, an object in the wave path that absorbs or reflects sound energy is subjected to the acoustic radiation force. The radiation force on a sphere or a cylinder has been studied extensively. A detailed theoretical work on a rigid sphere was presented by King [14] and extended [15] to include the effect of the sphere compressibility. Later, Hasegawa and Yosioka [16] provided theoretical and experimental work on the radiation force experienced by an isotropic elastic sphere. The acoustic radiation force on a rigid cylinder was also investigated [17] and extended to take into account its elasticity [18]. The effects of dissipative mechanisms, such as viscosity and heat conduction, were also studied and it was found that they drastically influence the acoustic radiation force [19].

The acoustic radiation force is usually a *steady* force, given that the intensity of the incident field does not change over time. It has been shown that the radiation force can also be *dynamic* (oscillatory), if the intensity of the incident field is modulated [20]. There are various ways to construct a modulated sound field. For example, one can use a single ultrasound beam whose amplitude is modulated at low frequency, or two interfering ultrasound beams driven at slightly different frequencies (dual beam mode), to produce a dynamic radiation force at their intersection. In the first case, the modulation of a single beam results in a field that is not spatially confined and exerts a dynamic radiation force on any object (including the transducer itself) that happens to be in the beam path. In the second case, the dynamic radiation force is confined to a small region where the two ultrasound beams intersect.

*Electronic addresses: mitri@ieee.org and mitri.farid@mayo.edu

Recently, the dynamic radiation force of ultrasound has been used to image the elasticity of an object, which could have great potential in medical diagnosis [21–24]. For example, in a new technique called vibro-acoustography, acoustic emissions from an object excited by the dynamic radiation force were used to reconstruct an image related to its mechanical properties (such as stiffness) [22]. This technique has been successfully used to image artery calcifications [22,25], breast micro-calcifications [26], calcium deposit on heart valves [27], human calcaneus and hip [28], and brachytherapy metal seeds [29,30]. More recently, the dynamic radiation force of ultrasound was also used to vibrate embedded spheres to estimate the shear modulus and viscosity of the medium in the neighborhood of the sphere [31]. In the field of material sciences the dynamic radiation force was used in determining resonance frequencies of differently shaped objects [32] and evaluating Young's modulus [33].

Despite the extensive use of the dynamic radiation force, very little work has been done on its theory. The aim of this work is to develop the theory of the *dynamic* acoustic radiation force, using a solid cylinder as an example. To the best of the authors' knowledge, the theoretical analysis of the dynamic radiation force on cylinders has never been studied before. We present the theory to calculate the dynamic radiation force on a solid cylinder insonified by two ultrasound waves driven at slightly different frequencies and interfering in a small region. It was assumed that the wave numbers of the incident waves are coplanar and the cylinder was placed entirely within that region. The dual beam acoustic scattering from the cylinder is solved first. Then analytical equations describing the dynamic components of radiation force are presented. The effects of longitudinal and shear waves' absorption inside the cylinder are also discussed. Numerical simulations are presented indicating the ways in which the dynamic radiation force function Y_d can be affected by the variations of the cylinder's mechanical parameters.

II. ACOUSTIC SCATTERING THEORY OF TWO PLANE WAVES FROM THE CYLINDER IN AN IDEAL FLUID

Usually, the process of computing the acoustic radiation force is divided into two steps: (1) solving the acoustic scattering problem, and (2) determining the radiation-stress tensor in the fluid. Following the work previously done [18], we derive the acoustic radiation force experienced by a solid cylinder excited by two plane waves; the velocity potential of the plane waves represented in cylindrical coordinates (r,θ,z) can be written as [34]

$$\phi_i = A\sum_{n=0}^{\infty} \varepsilon_n(-j)^n J_n(k_1 r)\cos(n\theta)e^{j\omega_1 t} + A\sum_{n=0}^{\infty} \varepsilon_n(-j)^n J_n(k_2 r)\cos(n\theta)e^{j\omega_2 t}, \quad (1)$$

where A is the amplitude, k_1 and k_2 are the wave numbers (denoted later by $k_i, i=1,2$), $J_n(k_i r)$ is the Bessel function of the first kind of order n and argument $k_i r$, and ε_n is defined by $\varepsilon_0=1$ and $\varepsilon_n=2$ $(n=1,2,3,\ldots)$.

The scattered waves may be expressed as

$$\phi_s = A\sum_{n=0}^{\infty} \varepsilon_n(-j)^n d_{1,n} H_n^{(2)}(k_1 r)\cos(n\theta)e^{j\omega_1 t} + A\sum_{n=0}^{\infty} \varepsilon_n(-j)^n d_{2,n} H_n^{(2)}(k_2 r)\cos(n\theta)e^{j\omega_2 t}, \quad (2)$$

where $H_n^{(2)}(k_i r)$ is the Hankel function of the second kind of order n and argument $k_i r$. The scattering coefficients are given by

$$d_{i,n} = \frac{-F_{i,n}J_n(x_i) + x_i J_n'(x_i)}{F_{i,n}H_n^{(2)}(x_i) - x_i H_n^{(2)'}(x_i)}, \quad i=1,2, \quad (3)$$

where $x_i = k_i a$, a being the radius of the cylinder. We define the coefficients $\alpha_{i,n}$ and $\beta_{i,n}$ as the real and imaginary parts of $d_{i,n}$, respectively.

The coefficients $F_{i,n}$ are given by

$$F_{i,n} = \frac{x_{i,2}^2 \rho}{2\rho^*}\left[\frac{A_n - B_n}{C_n - D_n}\right], \quad (4)$$

where ρ and ρ^* are the densities of the fluid and the cylinder, respectively, $x_{i,1}=x_i c/c_1$, $x_{i,2}=x_i c/c_2$, c is the speed of sound in fluid, and c_1 and c_2 are the longitudinal and shear wave velocities inside the cylinder material, respectively, with

$$A_n = \frac{\Lambda_n(x_{i,1})}{\Lambda_n(x_{i,1})+1}; \quad B_n = \frac{n^2}{\Lambda_n(x_{i,2}) + n^2 - \frac{1}{2}x_{i,2}^2};$$

$$C_n = \frac{\Lambda_n(x_{i,1}) + n^2 - \frac{1}{2}x_{i,2}^2}{\Lambda_n(x_{i,1})+1}; \quad (5)$$

$$D_n = \frac{n^2(\Lambda_n(x_{i,2})+1)}{\Lambda_n(x_{i,2}) + n^2 - \frac{1}{2}x_{i,2}^2};$$

where $\Lambda_n(x_{i,k}) = [-x_{i,k}J_n'(x_{i,k})/J_n(x_{i,k})]$, $i=1,2$, $k=1,2$.

The total velocity potential is then

$$\phi = \phi_i + \phi_s = A\sum_{n=0}^{\infty} \varepsilon_n(-j)^n [U_{1,n}(k_1 r) + jV_{1,n}(k_1 r)]\cos(n\theta)e^{j\omega_1 t} + A\sum_{n=0}^{\infty} \varepsilon_n(-j)^n [U_{2,n}(k_2 r) + jV_{2,n}(k_2 r)]\cos(n\theta)e^{j\omega_2 t}, \quad (6)$$

where $U_{1,n}, V_{1,n}, U_{2,n}, V_{2,n}$ and their derivatives are defined as

$$U_{1,n} = (1+\alpha_{1,n})J_n(k_1 r) + \beta_{1,n}Y_n(k_1 r),$$

$$U_{2,n} = (1+\alpha_{2,n})J_n(k_2 r) + \beta_{2,n}Y_n(k_2 r),$$

$$U_{l,n}' = \frac{d[U_{1,n}(k_1 r)]}{d[k_1 r]},$$

$$U_{2,n}' = \frac{d[U_{2,n}(k_2 r)]}{d[k_2 r]}, \quad (7)$$

$$V_{1,n} = \beta_{1,n}J_n(k_1 r) - \alpha_{1,n}Y_n(k_1 r),$$

$$V_{2,n} = \beta_{2,n}J_n(k_2 r) - \alpha_{2,n}Y_n(k_2 r),$$

$$V_{1,n}' = \frac{d[V_{1,n}(k_1 r)]}{d[k_1 r]},$$

$$V_{2,n}' = \frac{d[V_{2,n}(k_2 r)]}{d[k_2 r]}.$$

From both Eqs. (6) and (7) we have

$$\Psi = \mathrm{Re}[\phi] = A\sum_{n=0}^{\infty} \varepsilon_n R_n \cos(n\theta), \quad (8)$$

and R_n is expressed by

$$R_n = \mathrm{Re}[(-j)^n [U_{1,n}(k_1 r) + jV_{1,n}(k_1 r)]e^{j\omega_1 t} + (-j)^n \times [U_{2,n}(k_2 r) + jV_{2,n}(k_2 r)]e^{j\omega_2 t}]. \quad (9)$$

III. DYNAMIC RADIATION FORCE EXPERIENCED BY THE CYLINDER

The radiation force is calculated by averaging the net force on the cylinder over time. To compute the dynamic component of the radiation force, the assumption in this case

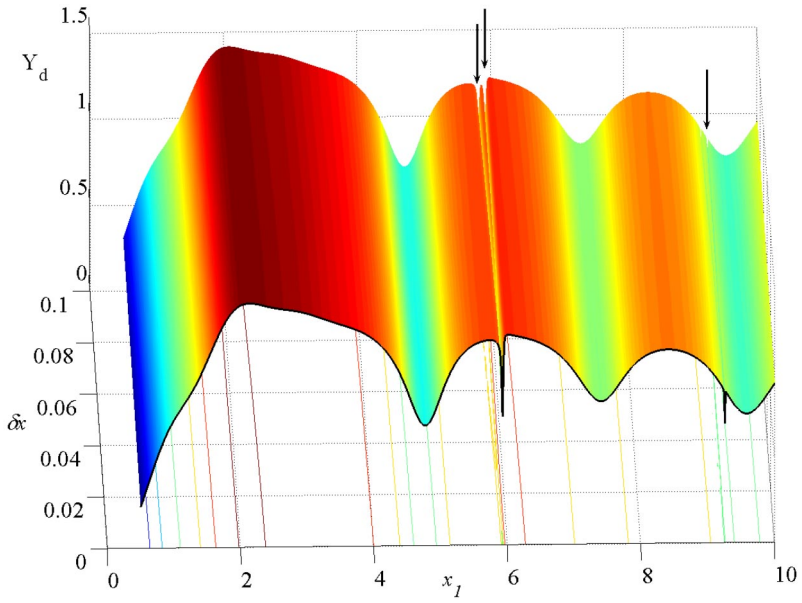

FIG. 1. (Color online) The dynamic radiation force function $(Y_d(x_1,x_2))$ curve for an aluminum cylinder in water. The minimum at $x_1=6$ and $\delta x=0$ is split into two minima while varying $\delta x(0\leqslant\delta x\leqslant 0.1)$. The black arrows point to the splitting of the resonance peaks.

is that $|\omega_1-\omega_2|\ll\omega_1+\omega_2$ so that the radiation force has a slow time variation at the low-frequency $\Delta\omega$. To discriminate this slow variation from the total radiation force, we use the short-term time average of an arbitrary function $\chi(t)$ over the interval of T at time t, defined as $\langle\chi(t)\rangle=(1/T)\int_{t-T/2}^{t+T/2}\chi(t)dt$ [35], where $2\pi/(\omega_1+\omega_2)\ll T\ll 2\pi/|\omega_1-\omega_2|$.

Thus, it can be proved that

$$\begin{aligned}\langle R_nR_{n+1}\rangle &= \tfrac{1}{2}(U_{1,n}V_{1,n+1}+U_{2,n}V_{2,n+1}-V_{1,n}U_{1,n+1}\\ &\quad -V_{2,n}U_{2,n+1})+\tfrac{1}{2}(U_{1,n}U_{2,n+1}-U_{2,n}U_{1,n+1}\\ &\quad +V_{1,n}V_{2,n+1}-V_{2,n}V_{1,n+1})\sin(\Delta\omega t)+\tfrac{1}{2}(U_{1,n}V_{2,n+1}\\ &\quad +U_{2,n}V_{1,n+1}-V_{1,n}U_{2,n+1}-V_{2,n}U_{1,n+1})\cos(\Delta\omega t),\end{aligned} \tag{10}$$

$$\begin{aligned}\langle R'_nR'_{n+1}\rangle|_{k_lr} &= \tfrac{1}{2}(U'_{1,n}V'_{1,n+1}+U'_{2,n}V'_{2,n+1}-V'_{1,n}U'_{1,n+1}\\ &\quad -V'_{2,n}U'_{2,n+1})+\tfrac{1}{2}(U'_{1,n}U'_{2,n+1}-U'_{2,n}U'_{1,n+1}\\ &\quad +V'_{1,n}V'_{2,n+1}-V'_{2,n}V'_{1,n+1})\sin(\Delta\omega t)\\ &\quad +\tfrac{1}{2}(U'_{1,n}V'_{2,n+1}+U'_{2,n}V'_{1,n+1}-V'_{1,n}U'_{2,n+1}\\ &\quad -V'_{2,n}U'_{1,n+1})\cos(\Delta\omega t),\end{aligned}$$

$$\begin{aligned}\langle R_nR'_{n+1}\rangle|_{k_lr} &= \tfrac{1}{2}(U_{1,n}V'_{1,n+1}+U_{2,n}V'_{2,n+1}-V_{1,n}U'_{1,n+1}\\ &\quad -V_{2,n}U'_{2,n+1})+\tfrac{1}{2}(U_{1,n}U'_{2,n+1}-U_{2,n}U'_{1,n+1}\\ &\quad +V_{1,n}V'_{2,n+1}-V_{2,n}V'_{1,n+1})\sin(\Delta\omega t)\\ &\quad +\tfrac{1}{2}(U_{1,n}V'_{2,n+1}+U_{2,n}V'_{1,n+1}-V_{1,n}U'_{2,n+1}\\ &\quad -V_{2,n}U'_{1,n+1})\cos(\Delta\omega t),\end{aligned}$$

$$\begin{aligned}\langle R'_nR_{n+1}\rangle|_{k_lr} &= \tfrac{1}{2}(U'_{1,n}V_{1,n+1}+U'_{2,n}V_{2,n+1}-V'_{1,n}U_{1,n+1}\\ &\quad -V'_{2,n}U_{2,n+1})+\tfrac{1}{2}(U'_{1,n}U_{2,n+1}-U'_{2,n}U_{1,n+1}\\ &\quad +V'_{1,n}V_{2,n+1}-V'_{2,n}V_{1,n+1})\sin(\Delta\omega t)\\ &\quad +\tfrac{1}{2}(U'_{1,n}V_{2,n+1}+U'_{2,n}V_{1,n+1}-V'_{1,n}U_{2,n+1}\\ &\quad -V'_{2,n}U_{1,n+1})\cos(\Delta\omega t).\end{aligned}$$

The radiation force per unit length $\langle F\rangle$ in the direction of the wave propagation is expressed by

$$\langle F\rangle=\langle F_r\rangle+\langle F_\theta\rangle+\langle F_{r,\theta}\rangle+\langle F_t\rangle, \tag{11}$$

where

$$\begin{aligned}\langle F_r\rangle &= \left\langle -\frac{1}{2}a\rho\int_0^{2\pi}\left(\frac{\partial\Psi}{\partial r}\right)^2_{r=a}\cos\theta\,d\theta\right\rangle\\ &= -2\pi a\rho|A|^2\sum_{n=0}^{\infty}\langle R'_nR'_{n+1}\rangle|_{r=a}\\ &= -\frac{\pi\rho|A|^2}{a}\Bigg[\sum_{n=0}^{\infty}[x_1^2(U'_{1,n}V'_{1,n+1}-V'_{1,n}U'_{1,n+1})\\ &\quad +x_2^2(U'_{2,n}V'_{2,n+1}-V'_{2,n}U'_{2,n+1})+x_1x_2(U'_{1,n}U'_{2,n+1}\\ &\quad -U'_{2,n}U'_{1,n+1}+V'_{1,n}V'_{2,n+1}-V'_{2,n}V'_{1,n+1})\sin(\Delta\omega t)\\ &\quad +x_1x_2(U'_{1,n}V'_{2,n+1}+U'_{2,n}V'_{1,n+1}-V'_{1,n}U'_{2,n+1}\\ &\quad -V'_{2,n}U'_{1,n+1})\cos(\Delta\omega t)]\Bigg],\end{aligned} \tag{12}$$

$$\langle F_\theta \rangle = \left\langle \frac{1}{2a}\rho \int_0^{2\pi} \left(\frac{\partial \Psi}{\partial \theta}\right)_{r=a}^2 \cos\theta \, d\theta \right\rangle$$

$$= \frac{2\pi\rho|A|^2}{a} \sum_{n=0}^{\infty} n(n+1)\langle R_n R_{n+1}\rangle$$

$$= \frac{\pi\rho|A|^2}{a}\Bigg[\sum_{n=0}^{\infty} n(n+1)((U_{1,n}V_{1,n+1} + U_{2,n}V_{2,n+1} - V_{1,n}U_{1,n+1} - V_{2,n}U_{2,n+1}) + (U_{1,n}U_{2,n+1} - U_{2,n}U_{1,n+1} + V_{1,n}V_{2,n+1}$$

$$- V_{2,n}V_{1,n+1})\sin(\Delta\omega t) + (U_{1,n}V_{2,n+1} + U_{2,n}V_{1,n+1} - V_{1,n}U_{2,n+1} - V_{2,n}U_{1,n+1})\cos(\Delta\omega t)) \Bigg], \tag{13}$$

$$\langle F_{r,\theta} \rangle = \left\langle \rho \int_0^{2\pi} \left(\frac{\partial \Psi}{\partial r}\right)_{r=a} \left(\frac{\partial \Psi}{\partial \theta}\right)_{r=a} \sin\theta \, d\theta \right\rangle$$

$$= 2\pi\rho|A|^2 \sum_{n=0}^{\infty} [n\langle R_n R'_{n+1}\rangle|_{r=a} - (n+1)\langle R'_n R_{n+1}\rangle|_{r=a}]$$

$$= \frac{\pi\rho|A|^2}{a} \sum_{n=0}^{\infty} \{n[(x_1 U_{1,n} V'_{1,n+1} + x_2 U_{2,n} V'_{2,n+1} - x_1 V_{1,n} U'_{1,n+1} - x_2 V_{2,n} U'_{2,n+1}) + (x_2 U_{1,n} U'_{2,n+1} - x_1 U_{2,n} U'_{1,n+1} + x_2 V_{1,n} V'_{2,n+1}$$

$$- x_1 V_{2,n} V'_{1,n+1})\sin(\Delta\omega t) + (x_2 U_{1,n} V'_{2,n+1} + x_1 U_{2,n} V'_{1,n+1} - x_2 V_{1,n} U'_{2,n+1} - x_1 V_{2,n} U'_{1,n+1})\cos(\Delta\omega t)]$$

$$- (n+1)[(x_1 U'_{1,n} V_{1,n+1} + x_2 U'_{2,n+1} V_{2,n+1} - x_1 V'_{1,n} U_{1,n+1} - x_2 V'_{2,n} U_{2,n+1}) + (x_1 U'_{1,n} U_{2,n+1} - x_2 U'_{2,n} U_{1,n+1}$$

$$+ x_1 V'_{1,n} V_{2,n+1} - x_2 V'_{2,n} V_{1,n+1})\sin(\Delta\omega t) + (x_1 U'_{1,n} V_{2,n+1} + x_2 U'_{2,n} V_{1,n+1} - x_1 V'_{1,n} U_{2,n+1} - x_2 V'_{2,n} U_{1,n+1})\cos(\Delta\omega t)]\}, \tag{14}$$

$$\langle F_t \rangle = \left\langle -\frac{1}{2c^2} a\rho \int_0^{2\pi} \left(\frac{\partial \Psi}{\partial t}\right)_{r=a}^2 \cos\theta \, d\theta \right\rangle$$

$$= -\frac{2\pi a\rho|A|^2}{c^2} \sum_{n=0}^{\infty} \left\langle \frac{\partial R_n}{\partial t} \frac{\partial R_{n+1}}{\partial t} \right\rangle$$

$$= -\frac{\pi\rho|A|^2}{a}\Bigg[\sum_{n=0}^{\infty} [x_1^2(U_{1,n}V_{1,n+1} - V_{1,n}U_{1,n+1})$$

$$+ x_2^2(U_{2,n}V_{2,n+1} - V_{2,n}U_{2,n+1}) + x_1 x_2(U_{1,n}U_{2,n+1}$$

$$- U_{2,n}U_{1,n+1} + V_{1,n}V_{2,n+1} - V_{2,n}V_{1,n+1})\sin(\Delta\omega t)$$

$$+ x_1 x_2(U_{1,n}V_{2,n+1} + U_{2,n}V_{1,n+1} - V_{1,n}U_{2,n+1}$$

$$- V_{2,n}U_{1,n+1})\cos(\Delta\omega t)] \Bigg]. \tag{15}$$

On the other hand, the velocity potential of the incident waves could be expressed with this form:

$$\phi_i = A\left(e^{j\omega_1 t} + e^{j\omega_2 t}\right). \tag{16}$$

The incident pressure can be expressed as

$$\tilde{P}_i(t) = \rho\frac{\partial \phi_i}{\partial t} = jA\rho\left(\omega_1 e^{j\omega_1 t} + \omega_2 e^{j\omega_2 t}\right). \tag{17}$$

The short-term time average of the energy is $\langle E(t)\rangle = \langle P_i^2(t)\rangle / \rho c^2$, where $P_i(t) = \mathrm{Re}[\tilde{P}_i(t)]$.

$$\left\langle P_i^2(t)\right\rangle = \frac{|A|^2\rho^2}{T}\int_{t-T/2}^{t+T/2} \left(\omega_1^2 \sin^2\omega_1 t + \omega_2^2 \sin^2\omega_2 t + 2\omega_1\omega_2 \sin\omega_1 t \sin\omega_2 t\right) dt,$$

$$\left\langle P_i^2(t)\right\rangle = |A|^2\rho^2\left(\frac{\omega_1^2}{2} + \frac{\omega_2^2}{2} + \omega_1\omega_2\cos(\Delta\omega t)\right). \tag{18}$$

The short-term time average of the energy becomes

$$\langle E(t)\rangle = \tfrac{1}{2}\rho k_1^2|A|^2 + \tfrac{1}{2}\rho k_2^2|A|^2 + \rho k_1 k_2|A|^2\cos(\Delta\omega t). \tag{19}$$

The radiation force for progressive waves is generally denoted by $\langle F\rangle = Y_p S_c \langle E\rangle$, where Y_ρ is a dimensionless factor called acoustic radiation force function and is the radiation force per unit energy density and unit cross-sectional surface, $\langle E\rangle$ is the mean energy density, and S_c is the cross-sectional area defined by the unit length of the cylinder multiplied by its diameter $(2a)$. Therefore,

$$2a\langle E\rangle = \rho k_1^2 a|A|^2 + \rho k_2^2 a|A|^2 + 2\rho k_1 k_2 a|A|^2\cos(\Delta\omega t)$$

and $\langle F\rangle$ is expressed by

$$\langle F\rangle = 2a\langle E_1\rangle Y_{p1} + 2a\langle E_2\rangle Y_{p2} + 2a\langle E_d\rangle Y_d. \tag{20}$$

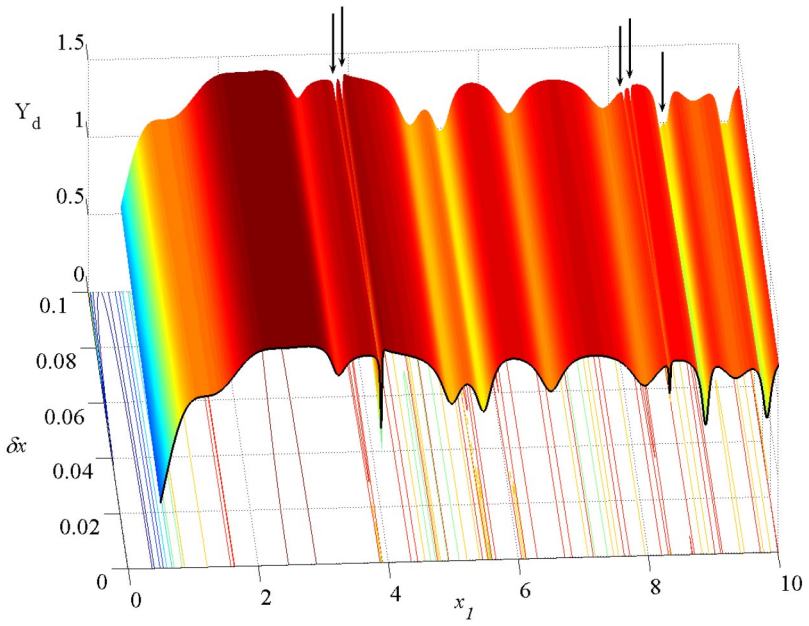

FIG. 2. (Color online) The dynamic radiation force function ($Y_d(x_1,x_2)$) curve for a brass cylinder in water. The splitting phenomenon is also observed at the minima of $Y_d(x_1,x_2)$. The black arrows point to the splitting of the resonance peaks

The final expression for the radiation force [i.e., Eq. (11)] is obtained after replacing $U_{1,n}, V_{1,n}, U_{2,n}, V_{2,n}$ and their derivatives in Eqs. (12)–(15) with the use of the following relations:

$$xZ_n'(x) = nZ_n(x) - xZ_{n+1}(x),$$

$$xZ_{n+1}'(x) = xZ_n(x) - (n+1)Z_{n+1}(x), \tag{21}$$

where $Z_n(x)$ stands for $J_n(x)$ or $Y_n(x)$ and

$$[J_{n+1}(x)Y_n(x) - J_n(x)Y_{n+1}(x)] = \frac{2}{\pi x}. \tag{22}$$

After some tough and tedious arithmetic manipulations, Eq. (11) can be greatly simplified to be

$$\begin{aligned}\langle F\rangle = {} & 2a\left(\tfrac{1}{2}\rho k_1^2|A|^2\right)Y_{p1} + 2a\left(\tfrac{1}{2}\rho k_2^2|A|^2\right)Y_{p2} \\ & + 2a(\rho k_1 k_2|A|^2)Y_3 \sin(\Delta\omega t) \\ & + 2a(\rho k_1 k_2|A|^2)Y_4 \cos(\Delta\omega t),\end{aligned} \tag{23}$$

where

$$Y_{p1} = -\frac{2}{x_1}\sum_{n=0}^{\infty}[\alpha_{1,n} + \alpha_{1,n+1} + 2\alpha_{1,n}\alpha_{1,n+1} + 2\beta_{1,n}\beta_{1,n+1}], \tag{24}$$

$$Y_{p2} = -\frac{2}{x_2}\sum_{n=0}^{\infty}[\alpha_{2,n} + \alpha_{2,n+1} + 2\alpha_{2,n}\alpha_{2,n+1} + 2\beta_{2,n}\beta_{2,n+1}], \tag{25}$$

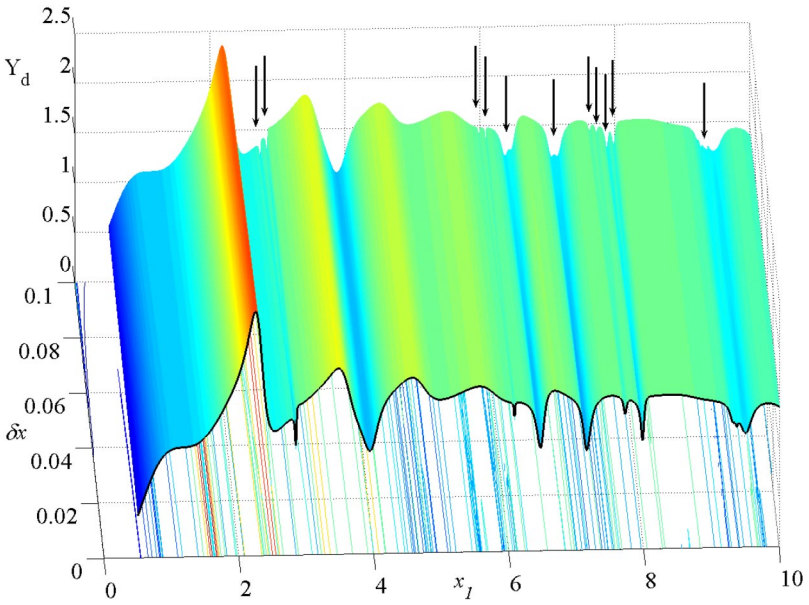

FIG. 3. (Color online) The dynamic radiation force function **(**$Y_d(x_1,x_2)$**)** curve for cadmium cylinder in water. Significant changes of the dynamic radiation force function occur at the function minima while varying δx. The black arrows point to the splitting of the resonance peaks.

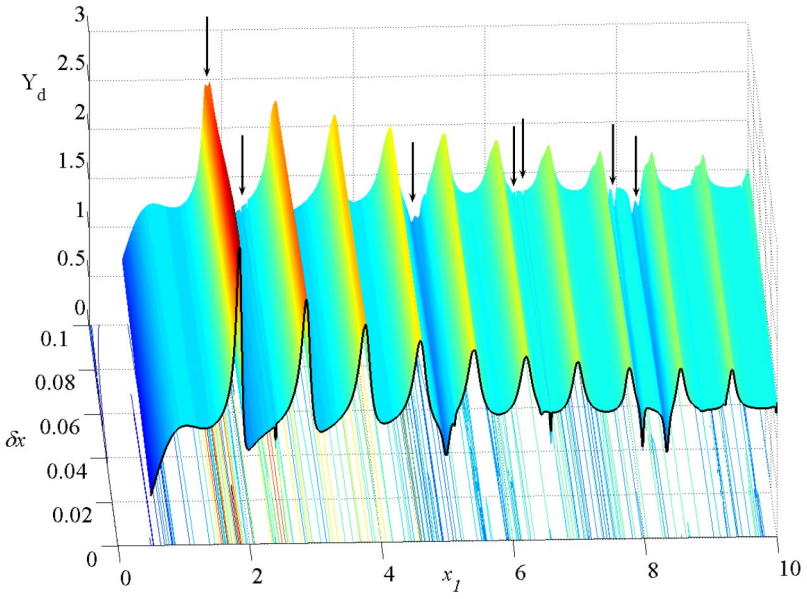

FIG. 4. (Color online) The dynamic radiation force function $(Y_d(x_1,x_2))$ curve for a gold cylinder in water. The black arrows point to the splitting of the resonance peaks.

$$Y_3 = \frac{\pi}{2}\sum_{n=0}^{\infty}\{[J_n(x_2)J_{n+1}(x_1) - J_n(x_1)J_{n+1}(x_2)](2 + \alpha_{1,n} + \alpha_{1,n+1} + \alpha_{2,n} + \alpha_{2,n+1}) + [J_n(x_2)Y_{n+1}(x_1) - Y_n(x_1)J_{n+1}(x_2)] \times (\beta_{1,n} + \beta_{1,n+1}) + [Y_n(x_2)J_{n+1}(x_1) - J_n(x_1)Y_{n+1}(x_2)] \times (\beta_{2,n} + \beta_{2,n+1}) + [J_n(x_2)J_{n+1}(x_1) - J_n(x_1)J_{n+1}(x_2) + Y_n(x_2)Y_{n+1}(x_1) - Y_n(x_1)Y_{n+1}(x_2)](\alpha_{1,n}\alpha_{2,n+1} + \alpha_{2,n}\alpha_{1,n+1} + \beta_{1,n}\beta_{2,n+1} + \beta_{2,n}\beta_{1,n+1}) + [J_n(x_2)Y_{n+1}(x_1) - Y_n(x_1)J_{n+1}(x_2) + J_n(x_1)Y_{n+1}(x_2) - Y_n(x_2)J_{n+1}(x_1)] \times (\alpha_{2,n}\beta_{1,n+1} + \beta_{1,n}\alpha_{2,n+1} - \alpha_{1,n}\beta_{2,n+1} - \beta_{2,n}\alpha_{1,n+1})\}, \quad (26)$$

$$Y_4 = \frac{\pi}{2}\sum_{n=0}^{\infty}\{[J_n(x_1)J_{n+1}(x_2) - J_n(x_2)J_{n+1}(x_1)] \times (\beta_{1,n} + \beta_{1,n+1} - \beta_{2,n} - \beta_{2,n+1}) + [J_n(x_2)Y_{n+1}(x_1) - Y_n(x_1)J_{n+1}(x_2)](\alpha_{1,n} + \alpha_{1,n+1}) + [J_n(x_1)Y_{n+1}(x_2) - Y_n(x_2)J_{n+1}(x_1)](\alpha_{2,n} + \alpha_{2,n+1}) + [J_n(x_2)Y_{n+1}(x_1) - Y_n(x_1)J_{n+1}(x_2) + J_n(x_1)Y_{n+1}(x_2) - Y_n(x_2)J_{n+1}(x_1)] \times (\alpha_{1,n}\alpha_{2,n+1} + \alpha_{2,n}\alpha_{1,n+1} + \beta_{1,n}\beta_{2,n+1} + \beta_{2,n}\beta_{1,n+1}) + [J_n(x_2)J_{n+1}(x_1) - J_n(x_1)J_{n+1}(x_2) + Y_n(x_2)Y_{n+1}(x_1) - Y_n(x_1)Y_{n+1}(x_2)](\alpha_{1,n}\beta_{2,n+1} + \beta_{2,n}\alpha_{1,n+1} - \beta_{1,n}\alpha_{2,n+1} - \alpha_{2,n}\beta_{1,n+1})\} \quad (27)$$

The first and second terms in Eq. (23) are the steady components of radiation force caused by each individual plane progressive wave while the third and the fourth represent the dynamic components of the force at the beating frequency.

The dynamic force can be rewritten as

$$\langle F_d\rangle = 2a\rho k_1 k_2 |A|^2\sqrt{Y_3^2 + Y_4^2}\cos(\Delta\omega t - \Phi) = 2a\langle E_d\rangle Y_d\cos(\Delta\omega t - \Phi), \quad (28)$$

where we define the dynamic energy density and dynamic radiation force function as

$$\langle E_d\rangle = \rho k_1 k_2 |A|^2, \quad (29)$$

$$Y_d = \sqrt{Y_3^2 + Y_4^2}. \quad (30)$$

The phase shift of the dynamic radiation force with respect to the incident field is given by $\Phi = \tan^{-1}(Y_3/Y_4)$.

A. Special cases

1. The frequencies of the incident plane waves are equal

When the frequencies of the incident plane waves are identical, $x_1 = x_2 = x, \alpha_{1,n} = \alpha_{2,n}, \beta_{1,n} = \beta_{2,n}$ and the incident waves are equivalent to a single plane wave with its amplitude doubled. Therefore its energy is quadrupled, hence the radiation force has four times higher amplitude. Equation (23) becomes

$$\langle F\rangle = 2a\left(\tfrac{1}{2}\rho k_1^2|A|^2\right)Y_{p1} + 2a\left(\tfrac{1}{2}\rho k_2^2|A|^2\right)Y_{p2} + 2a(\rho k_1 k_2|A|^2)Y_4 \quad (31)$$

and by using the wronksian [36] of the cylindrical Bessel functions [i.e., Eq. (22)], and from Eqs. (24)–(27), it can be verified that $Y_3 = 0$ and $Y_4 = Y_{p1} = Y_{p2} = Y_p$. Therefore, Eq. (31) becomes $\langle F\rangle = 4\left[2a\left(\frac{1}{2}\rho k^2|A|^2\right)Y_p\right]$ and the expression of Y_p is identical to the one given by Hasegawa *et al.* [18].

2. Effect of absorption

Absorption of sound (or ultrasound) in the cylinder material can be included by introducing complex wave numbers into the theory [37]. This principle can be directly applied to take into account compressional and shear wave absorption

TABLE I. Lossless materials' parameters used in the numerical calculations

Material	Mass density (10^3 kg/m^3)	Compressional velocity c_1 (m/s)	Shear velocity c_2 (m/s)
Aluminum	2.7	6420	3040
Brass	8.1	3830	2050
Cadmium	8.6	2780	1500
Gold	19.3	3240	1200

inside the cylinder material, especially for polymers. The normalized absorption coefficients of compressional (i.e., $\gamma_{i,1}$) and shear waves (i.e., $\gamma_{i,2}$), respectively, are constant quantities and independent of frequency, describing the behavior of many polymeric materials. In the theory described above, and for viscoelastic materials, the terms $x_{i,1}$ and $x_{i,2}$ are replaced by $\tilde{x}_{i,1}$ and $\tilde{x}_{i,2}$ given by

$$\tilde{x}_{i,1} = x_{i,1}(1 - j\gamma_{i,1}),$$
$$\tilde{x}_{i,2} = x_{i,2}(1 - j\gamma_{i,2}). \tag{32}$$

IV. NUMERICAL RESULTS

The $Y_d(x_1,x_2)$ relationship for an elastic cylinder in water was evaluated numerically by the use of Eq. (30) for different materials. The materials for which graphic results are shown in Figs. 1 through 4, and the values of the density and longitudinal and shear wave velocities used in the simulations are listed in Table I. These have all been assumed to be lossless materials immersed in water with a sound velocity of 1480 m s^{-1} and a density of 1000 Kg m^{-3}.

Three-dimensional plots of the $Y_d(x_1,x_2)$ function are performed and the results cover the range defined by the condition $|\omega_1-\omega_2| \ll \omega_1+\omega_2$ so that $\delta x = |x_1-x_2| \ll x_1+x_2$. Hence, the range is chosen by $0.5 \leqslant x_1 \leqslant 10$ and $0 \leqslant \delta x \leqslant 0.1$ in increments of 0.01. [The condition here is that when $\delta x \geqslant x_1$ or x_2, the dynamic component of the radiation force function $Y_d(x_1,x_2)$ is undefined.] It was verified that the shape of the $Y_d(x_1,x_2)$ curves does not vary significantly when the step value is decreased. The step value used in the calculations is extremely important because choosing a sufficiently small step allows capturing the resonance peaks that are very sharp.

TABLE II. Mechanical parameters of viscoelastic materials used in the numerical calculations.

Material	Mass density (kg/m^3)	Compressional velocity c_1(m/s)	Shear velocity c_2(m/s)	γ_1	γ_2
Lucite	1.191	2690	1340	0.0035	0.0053
Polyethylene	0.957	2430	950	0.0073	0.022

The special case where the frequencies of the incident plane waves are equal (i.e., $\delta x = 0$) is also shown in the figures (curve in bold), and the shape of $Y_d(x_1,x_2)$ corresponds to the steady radiation force function Y_p calculated by Hasegawa *et al.* [18].

Calculations of $Y_d(x_1,x_2)$ for two viscoelastic materials (lucite and polyethylene) were also evaluated. $Y_d(x_1,x_2)$ curves of these materials, listed in Table II with their specific parameters, are shown in Figs. 5 and 6, respectively. The assumption here is that $\gamma_{1,1}=\gamma_{2,1}=\gamma_1$ and $\gamma_{1,2}=\gamma_{2,2}=\gamma_2$, so that the compressional and shear absorption coefficients are the same for the first and second primary waves, respectively. The sound absorption was considered of constant amplitude versus frequency describing the behavior of many polymeric materials.

V. DISCUSSION

Equation (20) indicates that the total radiation force experienced by the cylinder is not the mere sum of the radiation

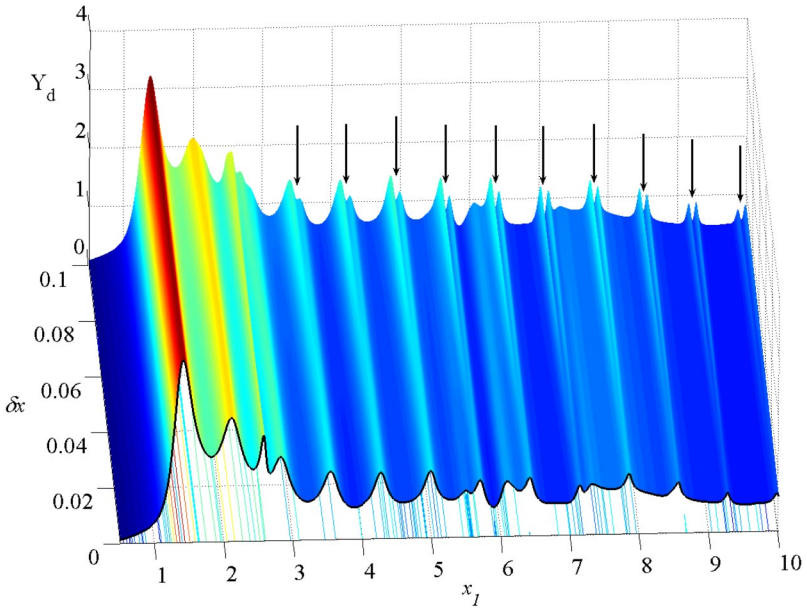

FIG. 5. (Color online) The dynamic radiation force function for an absorbent lucite cylinder immersed in water. The black arrows point to the splitting of the resonance peaks that is more prominent for this material.

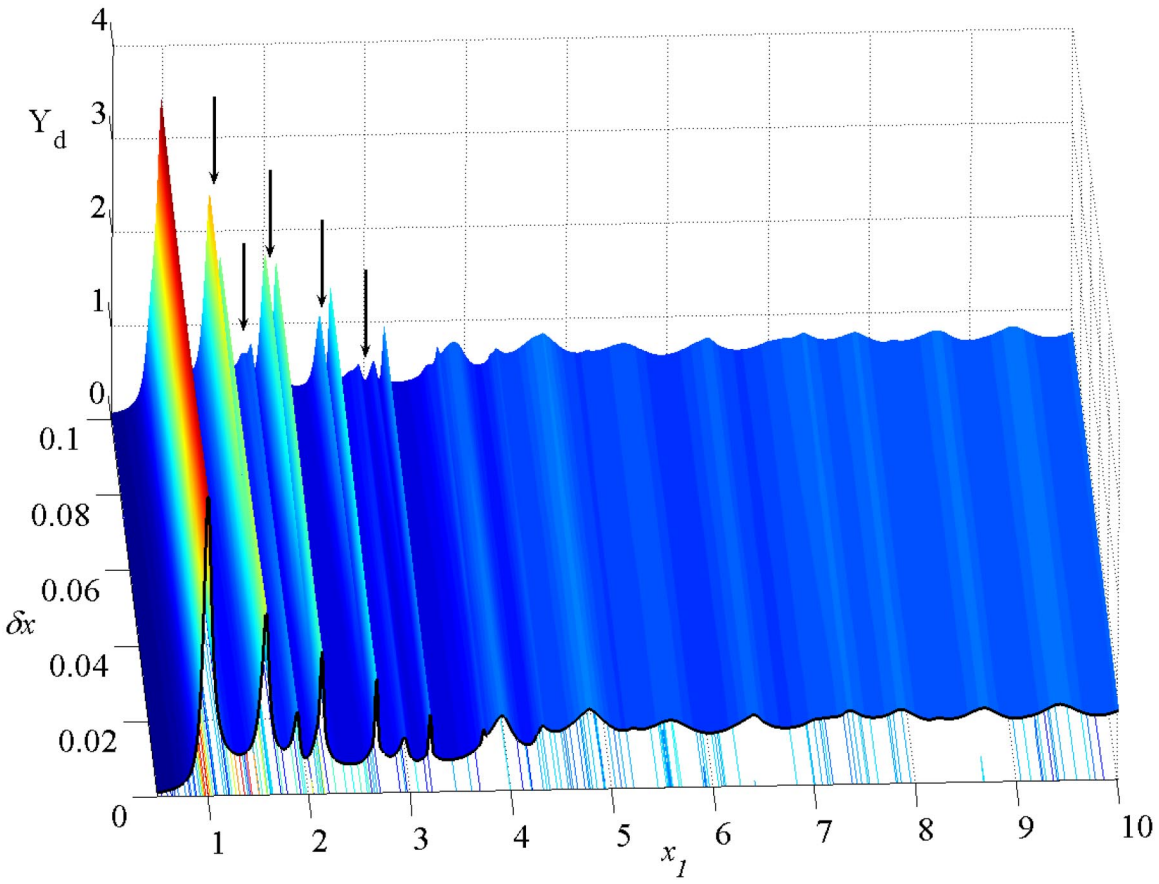

FIG. 6. (Color online) The same as in Fig. 5, but for an absorbent polyethylene cylinder. The damping of all peaks at high frequency appears more clearly for this material, whose absorption coefficients are greater than lucite.

forces due to each incident plane progressive wave. There is an additional term associated with the coupling between the two forces called the dynamic radiation force. Equation (28) shows that the dynamic radiation force is proportional to the cross-sectional area of the cylinder and the dynamic energy density, which is related to the intensity of the incident fields. The dynamic radiation force function $Y_d(x_1,x_2)$ is a coefficient determined by the scattering and absorption properties of the cylinder and its surrounding medium (in this case water). It is also a function of x_1 and x_2, and when x_1 approaches x_2 the expression of $Y_d(x_1,x_2)$ is reduced to the static radiation force function $Y_p(x)$ where only one single sound plane wave is presented.

Notice that in the section of the static radiation force function where the $Y_p(x)$ curve is relatively flat, we see very little change in $Y_d(x_1,x_2)$, so that $Y_d(x_1,x_2)$ could be approximated to $Y_p(x)$. However, when δx increases, the value of $Y_d(x_1,x_2)$ starts to deviate from $Y_p(x)$, which drastically change radiation force (Figs. 1–6). This effect is clearly shown in the figures at some maxima and minima of the curves. Hence, it is essential to use the expression of $Y_d(x_1,x_2)$ given by Eq. (30).

In the figures, the positions of minima and maxima are determined by the cylinder's material properties. In order to give a theoretical interpretation of these maxima and minima peaks in the $Y_d(x_1,x_2)$ curves, it is essential to introduce the concept of the scattering cross-section σ that characterizes the scattering strength of the cylinder, thus radiation force. When the incident wave strikes the elastic cylinder, it generates a surface wave that is propagated on its surface [38]. This wave decays progressively and reradiates a bulk wave in the fluid medium surrounding the cylinder. The resonances are the result of surface waves that reradiate scattered bulk waves in the fluid. Thus, maxima and minima peaks are both due to resonances of the solid cylinder.

The scattering of the incident wave is formerly due to the presence of the object along its path and this (scattering) profile is instantaneous. In addition, under the influence of the wave (transfer of momentum), the object itself begins to vibrate and produces a sound (or ultrasound) field, thus, additional acoustic scattering. Therefore, the total scattered amplitude may be considered as the sum of two contributions: the rigid contribution, which is the response of a totally impenetrable object, and the elastic contribution, which accounts for the resonances and depends on the shape and mechanical characteristics of the object. However, the total scattering cross section of the cylinder is not only the sum of the "rigid" and "elastic" scattering cross sections; there is an interference term between these two contributions [39]. Hence, when bulk waves are out of phase with the rigid term, resonance appears as minima instead of maxima peaks in the total scattering cross section curves. Moreover, the width of any resonance peak is related to the time in which surface

waves spend inside the cylinder to be transformed to bulk waves. This period is known as the "dwell time" [40]. So, for sharp peaks, surface waves are rapidly attenuated to create bulk waves.

VI. CONCLUSION

The major achievement of this work is to calculate theoretically the dynamic components of the radiation force experienced by a solid cylinder placed in an amplitude-modulated sound (or ultrasound) field (produced by interfering two ultrasound beams driven at slightly different frequencies), and immersed in a nonviscous fluid [i.e., Eq. (30)]. Analytical equations are derived and numerical calculations of the dynamic radiation force function are presented for elastic and viscoelastic materials. It is shown that the radiation force is no longer static and has an oscillatory component when the modulation increases, hence resulting in the splitting of some of the minima and maxima resonance peaks.

ACKNOWLEDGMENTS

The authors are grateful to Dr. M. Fatemi as well as Professor J. F. Greenleaf for numerous helpful comments.

[1] R. T. Beyer, J. Acoust. Soc. Am. **63**, 1025 (1978).
[2] A. Kundt, Ann. Phys. (Leipzig) **127**, 497 (1866).
[3] L. Rayleigh, Philos. Mag. **3**, 338 (1902).
[4] P. J. Westervelt, J. Acoust. Soc. Am. **23**, 312 (1951).
[5] P. J. Westervelt, J. Acoust. Soc. Am. **29**, 26 (1957).
[6] M. Barmatz and P. Collas, J. Acoust. Soc. Am. **77**, 928 (1985).
[7] C. P. Lee and T. G. Wang, J. Acoust. Soc. Am. **94**, 1099 (1993).
[8] Z. Y. Jiang and J. F. Greenleaf, J. Acoust. Soc. Am. **100**, 741 (1996).
[9] O. V. Rudenko, A. P. Sarvazyan, and S. Y. Emelianov, J. Acoust. Soc. Am. **99**, 2791 (1996).
[10] D. T. Brandt, Nature (London) **413**, 474 (2001).
[11] K. Beissner, J. Acoust. Soc. Am. **79**, 1610 (1986).
[12] B. T. Chu and R. E. Apfel, J. Acoust. Soc. Am. **72**, 1673 (1982).
[13] G. R. Torr, Am. J. Phys. **52**, 402 (1984).
[14] L. V. King, Proc. R. Soc. London, Ser. A **147**, 212 (1935).
[15] K. Yosioka and Y. Kawasima, Acustica **5**, 167 (1955).
[16] T. Hasegawa and K. Yosioka, J. Acoust. Soc. Am. **46**, 1139 (1969).
[17] J. Awatani, Mem. Inst. Sci. Ind. Res., Osaka Univ. **12**, 95 (1955).
[18] T. Hasegawa *et al.*, J. Acoust. Soc. Am. **83**, 1770 (1988).
[19] A. Doinikov, Phys. Rev. E **54**, 6297 (1996).
[20] M. Greenspan, R. F. Breckenridge, and C. E. Tschiegg, J. Acoust. Soc. Am. **63**, 1031 (1978).
[21] L. Gao *et al.*, J. Acoust. Soc. Am. **97**, 3875 (1995).
[22] M. Fatemi and J. F. Greenleaf, Science **280**, 82 (1998).
[23] A. P. Sarvazyan *et al.*, Ultrasound Med. Biol. **24**, 1419 (1998).
[24] S. Catheline, F. Wu, and M. Fink, J. Acoust. Soc. Am. **105**, 2941 (1999).
[25] X. M. Zhang *et al.*, J. Acoust. Soc. Am. **113**, 1249 (2003).
[26] M. Fatemi *et al.*, IEEE Trans. Med. Imaging **21**, 1 (2002).
[27] A. Alizad *et al.*, J. Am. Soc. Echocardiogr **15**, 1391 (2002).
[28] S. Callé *et al.*, Ultrasound Med. Biol. **29**, 465 (2003).
[29] F. G. Mitri, P. Trompette, and J. Y. Chapelon, IEEE Trans. Med. Imaging **23**, 1 (2004).
[30] F. G. Mitri, P. Trompette, and J. Y. Chapelon, Proc.-IEEE Ultrason. Symp. 1528 (2003).
[31] S. Chen, M. Fatemi, and J. F. Greenleaf, J. Acoust. Soc. Am. **112**, 884 (2002).
[32] F. G. Mitri, P. Trompette, and J. Y. Chapelon, J. Acoust. Soc. Am. **114**, 2648 (2003).
[33] M. Fatemi and J. F. Greenleaf, Ultrason. Imaging **21**, 141 (1999).
[34] J. J. Faran, J. Acoust. Soc. Am. **23**, 405 (1951).
[35] M. Fatemi and J. F. Greenleaf, Proc. Natl. Acad. Sci. U.S.A. **96**, 6603 (1999).
[36] M. Abramowitz and I. Stegun, *Handbook of Mathematical Functions* (Dover, New York, 1972).
[37] F. G. Mitri, Z. E. A. Fellah, and J. Y. Chapelon, J. Acoust. Soc. Am. **115**, 1411 (2004).
[38] N. Gespa, *Acoustic Scattering by Elastic Scatters with Simple Geometrical Shape* (Cedocar, Paris, 1987) (in French).
[39] A. Derode, A. Tourin, and M. Fink, Phys. Rev. E **64**, 036605 (2001).
[40] A. Lagendijk and B. A. Van Tiggelen, Phys. Rep. **270**, 143 (1996).